IRis

Northeastern University

Physics Faculty Publications

Department of Physics

January 01, 2008

Dijet signals for low mass strings at the LHC

Luis A. Anchordoqui
University of Wisconsin - Milwaukee

Haim Goldberg
Northeastern University

Dieter Lüst
Max-Planck-Institut für Physik, Germany; Ludwig-Maximilians-Universität, Germany

Satoshi Nawata
University of Wisconsin - Milwaukee

Stephan Stieberger
Max-Planck-Institut für Physik

See next page for additional authors

Recommended Citation

Anchordoqui, Luis A.; Goldberg, Haim; Lüst, Dieter; Nawata, Satoshi; Stieberger, Stephan; and Taylor, Tomasz T., "Dijet signals for low mass strings at the LHC" (2008). *Physics Faculty Publications.* Paper 128. http://hdl.handle.net/2047/d20000739

This work is available open access, hosted by Northeastern University.

Author(s)
Luis A. Anchordoqui, Haim Goldberg, Dieter Lüst, Satoshi Nawata, Stephan Stieberger, and Tomasz T. Taylor

This article is available at IRis: http://iris.lib.neu.edu/physics_fac_pubs/128

MPP–2008–86
LMU-ASC 42/08
NUB-3262-Th-08

Dijet signals for low mass strings at the LHC

Luis A. Anchordoqui,[1] Haim Goldberg,[2] Dieter Lüst,[3,4]
Satoshi Nawata,[1] Stephan Stieberger,[3] and Tomasz R. Taylor[2]

[1]*Department of Physics,*
University of Wisconsin-Milwaukee, Milwaukee, WI 53201, USA

[2]*Department of Physics,*
Northeastern University, Boston, MA 02115, USA

[3]*Max–Planck–Institut für Physik*
Werner–Heisenberg–Institut, 80805 München, Germany

[4]*Arnold Sommerfeld Center for Theoretical Physics*
Ludwig-Maximilians-Universität München, 80333 München, Germany

(Dated: August 2008)

arXiv:0808.0497v3 [hep-ph] 30 Jun 2010

Abstract

We consider extensions of the standard model based on open strings ending on D-branes, with gauge bosons due to strings attached to stacks of D-branes and chiral matter due to strings stretching between intersecting D-branes. Assuming that the fundamental string mass scale is in the TeV range and the theory is weakly coupled, we discuss possible signals of string physics at the Large Hadron Collider (LHC). In such D-brane constructions, the dominant contributions to full-fledged string amplitudes for all the common QCD parton subprocesses leading to dijets are completely independent of the details of compactification, and can be evaluated in a parameter-free manner. We make use of these amplitudes evaluated near the first resonant pole to determine the discovery potential of LHC for the first Regge excitations of the quark and gluon. Remarkably, the reach of LHC after a few years of running can be as high as 6.8 TeV. Even after the first 100 pb^{-1} of integrated luminosity, string scales as high as 4.0 TeV can be discovered. For string scales as high as 5.0 TeV, observations of resonant structures in $pp \to$ direct γ + jet can provide interesting corroboration for string physics at the TeV-scale.

Experiments at the Large Hadron Collider (LHC) will search for the Higgs boson – the last missing piece of the standard model. At the same time, searches will be conducted for signals of new physics beyond it. Although many extensions of the standard model have been proposed over the last thirty years, none of them has been favored so far by the experimental data. There are differences, however, between various models with respect to their testability in the energy range accessible at the LHC. It has recently become clear [1–4] that superstring theory offers one of the most robust scenarios beyond the standard model, provided that its fundamental mass scale is sufficiently "low", *i.e.* of order TeV. The purpose of this Letter is to discuss dijet signals of low mass string theory at the LHC and to determine the discovery reach based on the measurements of the corresponding cross sections.

The mass scale M_s of fundamental strings can be as low as few TeV provided that spacetime extends into large extra dimensions, allowing a novel solution for the hierarchy problem [5, 6]. This mass determines the center of mass energy threshold $\sqrt{s} \geq M_s$ for the production of Regge resonances in parton collisions, thus for the onset of string effects at the LHC [4]. (Mandelstam variables s, t, u used in this Letter refer to parton subprocesses.) We consider the extensions of the standard model based on open strings ending on D-branes, with gauge bosons due to strings attached to stacks of D-branes and chiral matter due to strings stretching between intersecting D-branes [7]. Only one assumption is necessary in order to set up a solid framework: the string coupling must be small in order to rely on perturbation theory in the computations of scattering amplitudes. In this case, black hole production and other strong gravity effects occur at energies above the string scale; therefore at least a few lowest Regge recurrences are available for examination, free from interference with some complex quantum gravitational phenomena. Starting from a small string coupling, the values of standard model coupling constants are determined by D-brane configurations and the properties of extra dimensions, hence that part of superstring theory requires intricate model-building; however, as argued in Refs. [1–4], some basic properties of Regge resonances like their production rates and decay widths are completely model-independent. The resonant character of parton cross sections should be easy to detect at the LHC if the string mass scale is not too high. Direct photon production channels discussed in [1, 2] are very interesting because the signal is due to processes that are absent in the standard model at the leading (tree level) order of perturbation theory. On the other hand, dijet production is a standard tree-level QCD process. However, as argued in this Letter, the presence of string resonances may lead to a dramatic enhancement of the production rates and allow access to higher string mass scales. In addition, dijet calculations do not depend on the unknown mixing parameter characterizing the embedding of hypercharge in the extended D-brane gauge group. Moreover, as discussed later in this work, future measurements of dijet angular distributions can provide a potent method for distinguishing between various compactification scenarios.

The physical processes underlying dijet production at the LHC are the collisions of two partons, producing two final partons that fragment into hadronic jets. The corresponding $2 \to 2$ scattering amplitudes, computed at the leading order in string perturbation theory, are collected in Ref. [4]. The amplitudes involving four gluons as well as those with two gluons plus two quarks do not depend on the compactification details and are completely model-independent. All string effects are encapsulated in these amplitudes in one "form factor" function of Mandelstam variables $s,\ t,\ u$ (constrained by $s+t+u=0$):

$$V(s,t,u) = \frac{s\,u}{tM_s^2} B(-s/M_s^2, -u/M_s^2) = \frac{\Gamma(1-s/M_s^2)\,\Gamma(1-u/M_s^2)}{\Gamma(1+t/M_s^2)}. \tag{1}$$

The physical content of the form factor becomes clear after using the well-known expansion in terms of s-channel resonances [8]:

$$B(-s/M_s^2, -u/M_s^2) = -\sum_{n=0}^{\infty} \frac{M_s^{2-2n}}{n!} \frac{1}{s - nM_s^2} \left[\prod_{J=1}^{n} (u + M_s^2 J) \right], \tag{2}$$

which exhibits s-channel poles associated to the propagation of virtual Regge excitations with masses $\sqrt{n} M_s$. Thus near the nth level pole ($s \to nM_s^2$):

$$V(s,t,u) \approx \frac{1}{s - nM_s^2} \times \frac{M_s^{2-2n}}{(n-1)!} \prod_{J=0}^{n-1} (u + M_s^2 J) \ . \tag{3}$$

In specific amplitudes, the residues combine with the remaining kinematic factors, reflecting the spin content of particles exchanged in the s-channel, ranging from $J = 0$ to $J = n + 1$.

The amplitudes for the four-fermion processes like quark-antiquark scattering are more complicated because the respective form factors describe not only the exchanges of Regge states but also of heavy Kaluza-Klein and winding states with a model-dependent spectrum determined by the geometry of extra dimensions. Fortunately, they are suppressed, for two reasons. First, the QCD $SU(3)$ color group factors favor gluons over quarks in the initial state. Second, the parton luminosities in proton-proton collisions at the LHC, at the parton center of mass energies above 1 TeV, are significantly lower for quark-antiquark subprocesses than for gluon-gluon and gluon-quark [2]. The collisions of valence quarks occur at higher luminosity; however, there are no Regge recurrences appearing in the s-channel of quark-quark scattering [4].

Before proceeding, we pause to present our notation. The first Regge excitations of the gluon (g) and quarks (q) will be denoted by g^*, q^*, respectively. In the D-brane models under consideration, the ordinary $SU(3)$ color gauge symmetry is extended to $U(3)$, so that the open strings terminating on the stack of "color" branes contain an additional $U(1)$ gauge boson C and its excitations to accompany the gluon and its excitations. The first excitation of the C will be denoted by C^*.

In the following we isolate the contribution to the partonic cross section from the first resonant state. Note that far below the string threshold, at partonic center of mass energies $\sqrt{s} \ll M_s$, the form factor $V(s,t,u) \approx 1 - \frac{\pi^2}{6} su/M_s^4$ [4] and therefore the contributions of Regge excitations are strongly suppressed. The s-channel pole terms of the average square amplitudes contributing to dijet production at the LHC can be obtained from the general formulae given in Ref. [4], using Eq.(3). However, for phenomenological purposes, the poles need to be softened to a Breit-Wigner form by obtaining and utilizing the correct *total* widths of the resonances [3]. After this is done, the contributions of the various channels are as follows:

$$\begin{aligned} |\mathcal{M}(gg \to gg)|^2 \ = \ & \frac{19}{12} \frac{g^4}{M_s^4} \left\{ W_{g^*}^{gg \to gg} \left[\frac{M_s^8}{(s - M_s^2)^2 + (\Gamma_{g^*}^{J=0} \ M_s)^2} + \frac{t^4 + u^4}{(s - M_s^2)^2 + (\Gamma_{g^*}^{J=2} \ M_s)^2} \right] \right. \\ & \left. + \ W_{C^*}^{gg \to gg} \left[\frac{M_s^8}{(s - M_s^2)^2 + (\Gamma_{C^*}^{J=0} \ M_s)^2} + \frac{t^4 + u^4}{(s - M_s^2)^2 + (\Gamma_{C^*}^{J=2} \ M_s)^2} \right] \right\}, \end{aligned} \tag{4}$$

$$\begin{aligned} |\mathcal{M}(gg \to q\bar{q})|^2 \ = \ & \frac{7}{24} \frac{g^4}{M_s^4} \ N_f \ \left[W_{g^*}^{gg \to q\bar{q}} \frac{ut(u^2 + t^2)}{(s - M_s^2)^2 + (\Gamma_{g^*}^{J=2} \ M_s)^2} \right. \\ & \left. + \ W_{C^*}^{gg \to q\bar{q}} \frac{ut(u^2 + t^2)}{(s - M_s^2)^2 + (\Gamma_{C^*}^{J=2} \ M_s)^2} \right] \end{aligned} \tag{5}$$

$$|\mathcal{M}(q\bar{q}\to gg)|^2 = \frac{56}{27}\frac{g^4}{M_s^4}\left[W_{g^*}^{q\bar{q}\to gg}\frac{ut(u^2+t^2)}{(s-M_s^2)^2+(\Gamma_{g^*}^{J=2}\ M_s)^2} + W_{C^*}^{q\bar{q}\to gg}\frac{ut(u^2+t^2)}{(s-M_s^2)^2+(\Gamma_{C^*}^{J=2}\ M_s)^2}\right], \tag{6}$$

$$|\mathcal{M}(qg\to qg)|^2 = -\frac{4}{9}\frac{g^4}{M_s^2}\left[\frac{M_s^4 u}{(s-M_s^2)^2+(\Gamma_{q^*}^{J=1/2}\ M_s)^2}+\frac{u^3}{(s-M_s^2)^2+(\Gamma_{q^*}^{J=3/2}\ M_s)^2}\right], \tag{7}$$

where g is the QCD coupling constant ($\alpha_{\rm QCD}=\frac{g^2}{4\pi}\approx 0.1$) and $\Gamma_{g^*}^{J=0}=75\,(M_s/\text{TeV})$ GeV, $\Gamma_{C^*}^{J=0}=150\,(M_s/\text{TeV})$ GeV, $\Gamma_{g^*}^{J=2}=45\,(M_s/\text{TeV})$ GeV, $\Gamma_{C^*}^{J=2}=75\,(M_s/\text{TeV})$ GeV, $\Gamma_{q^*}^{J=1/2}=\Gamma_{q^*}^{J=3/2}=37\,(M_s/\text{TeV})$ GeV are the total decay widths for intermediate states g^*, C^*, and q^* (with angular momentum J) [3]. The associated weights of these intermediate states are given in terms of the probabilities for the various entrance and exit channels

$$W_{g^*}^{gg\to gg}=\frac{8(\Gamma_{g^*\to gg})^2}{8(\Gamma_{g^*\to gg})^2+(\Gamma_{C^*\to gg})^2}=0.44\,, \tag{8}$$

$$W_{C^*}^{gg\to gg}=\frac{(\Gamma_{C^*\to gg})^2}{8(\Gamma_{g^*\to gg})^2+(\Gamma_{C^*\to gg})^2}=0.56\,, \tag{9}$$

$$W_{g^*}^{gg\to q\bar{q}}=W_{g^*}^{q\bar{q}\to gg}=\frac{8\,\Gamma_{g^*\to gg}\,\Gamma_{g^*\to q\bar{q}}}{8\,\Gamma_{g^*\to gg}\,\Gamma_{g^*\to q\bar{q}}+\Gamma_{C^*\to gg}\,\Gamma_{C^*\to q\bar{q}}}=0.71\,, \tag{10}$$

$$W_{C^*}^{gg\to q\bar{q}}=W_{C^*}^{q\bar{q}\to gg}=\frac{\Gamma_{C^*\to gg}\,\Gamma_{C^*\to q\bar{q}}}{8\,\Gamma_{g^*\to gg}\,\Gamma_{g^*\to q\bar{q}}+\Gamma_{C^*\to gg}\,\Gamma_{C^*\to q\bar{q}}}=0.29\,. \tag{11}$$

Superscripts $J=2$ are understood to be inserted on all the Γ's in Eqs.(8), (9), (10), (11). Equation (4) reflects the fact that weights for $J=0$ and $J=2$ are the same [3]. In what follows we set the number of flavors $N_f=6$.

The resonance would be visible in data binned according to the invariant mass M of the dijet, after setting cuts on the different jet rapidities, $|y_1|$, $|y_2|\leq 1$ [9] and transverse momenta $p_{\rm T}^{1,2}>50$ GeV. In Fig. 1 we show a representative plot of the invariant mass spectrum, for $M_s=2$ TeV, detailing the contribution of each subprocess. The QCD background has been calculated at the partonic level from the same processes as designated for the signal, with the addition of $qq\to qq$ and $q\bar{q}\to q\bar{q}$. Our calculation, making use of the CTEQ6D parton distribution functions [10] agrees with that presented in [9].

We now estimate (at the parton level) the LHC discovery reach. Standard bump-hunting methods, such as obtaining cumulative cross sections, $\sigma(M_0)=\int_{M_0}^{\infty}\frac{d\sigma}{dM}\,dM$, from the data and searching for regions with significant deviations from the QCD background, may reveal an interval of M suspected of containing a bump. With the establishment of such a region, one may calculate a signal-to-noise ratio, with the signal rate estimated in the invariant mass window $[M_s-2\Gamma,\ M_s+2\Gamma]$. The noise is defined as the square root of the number of background events in the same dijet mass interval for the same integrated luminosity.

The top two and bottom curves in Fig. 1 show the behavior of the signal-to-noise (S/N) ratio as a function of the string scale for three integrated luminosities (100 fb^{-1}, 30 fb^{-1} and 100 pb^{-1}) at the LHC. It is remarkable that within 1-2 years of data collection, *string scales as large as 6.8 TeV are open to discovery at the* $\geq 5\sigma$ *level.* For 30 fb^{-1}, the presence of a resonant state with mass as large as 5.7 TeV can provide a signal of convincing significance

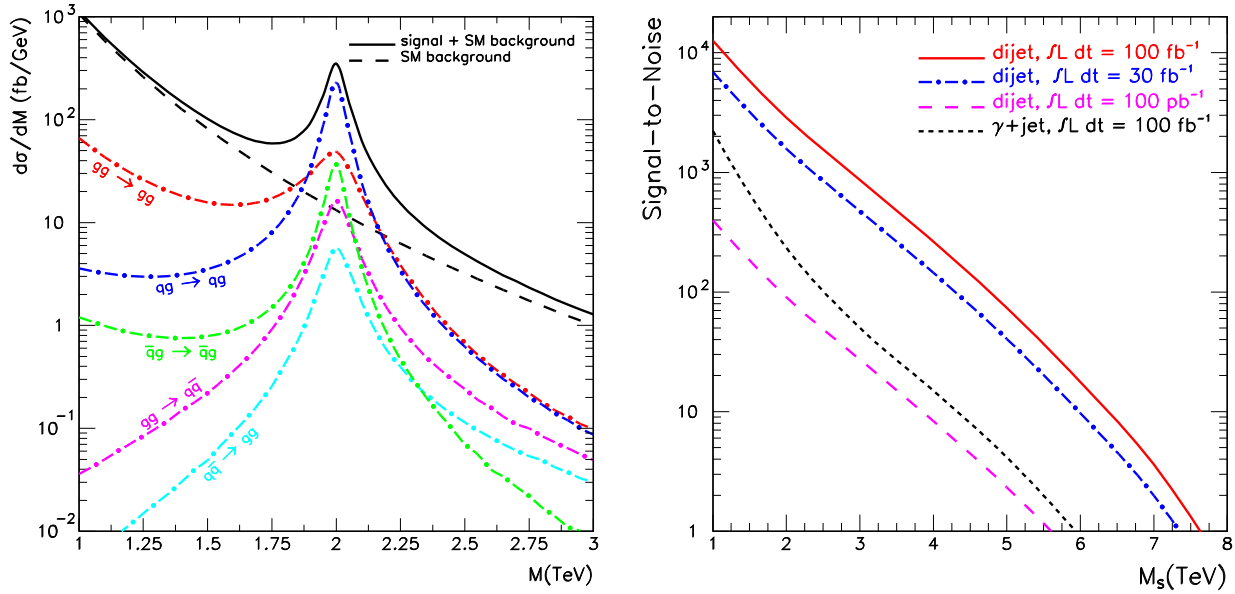

FIG. 1: *Left panel:* $d\sigma/dM$ (units of fb/GeV) *vs.* M (TeV) is plotted for the case of SM QCD background (dashed line) and (first resonance) string signal + background (solid line). The dot-dashed lines indicate the different contributions to the string signal ($gg \to gg$, $gg \to q\bar{q}$, $qg \to qg$, and $q\bar{q} \to gg$). *Right panel:* $pp \to$ dijet signal-to-noise ratio for three integrated luminosities. For comparison, we also show the signal-to-noise of $pp \to \gamma + \text{jet}$, for $\kappa^2 \simeq 0.02$, see Ref. [1].

($S/N = 592/36 > 13$). The bottom curve, corresponding to data collected in a very early run of 100 pb^{-1}, shows that a resonant mass as large as 4.0 TeV can be observed with 10σ significance! Once more, we stress that these results contain no unknown parameters. They depend only on the D-brane construct for the standard model, and *are independent of compactification details.*

For comparison with our previous analysis, we also show in Fig. 1 a fourth curve, for the process $pp \to \gamma+$ jet. (In what follows, γ refers to an isolated gamma ray.) In Ref. [2] a cut ($p_T^\gamma > 300$ GeV) was selected for discovery of new physics. As far as the signal is concerned, this cut is largely equivalent to selecting on γ-jet invariant masses in the 2-5 TeV range, with cuts on photon and jet rapidities $|y_1|$, $|y_2| < 2.4$ [11]. However, for $M_s > 2$ TeV the background is greatly reduced with the dijet mass method used here, resulting in an extension of the discovery reach, up to about 5 TeV [12]. The signal used to obtain the results displayed in Fig. 1 includes the parton subprocesses $gg \to g\gamma$ (which does not exist at tree level in QCD, and which was the only subprocess evaluated in [1, 2]), $qg \to q\gamma$, $\bar{q}g \to \bar{q}\gamma$, and $q\bar{q} \to g\gamma$. All except the first have been calculated in QCD and constitute the standard model background. The projection of the photon onto the C gauge boson was also effected in the last-cited references. Although the discovery reach is not as high as that for dijets, the measurement of $pp \to \gamma + \text{jet}$ can potentially provide an interesting corroboration for the stringy origin for new physics manifest as a resonant structure in LHC data.

We now turn to the analysis of the angular distributions. QCD parton-parton cross sections are dominated by t-channel exchanges that produce dijet angular distributions which peak at small center of mass scattering angles. In contrast, non–standard contact interactions or excitations of resonances result in a more isotropic distribution. In terms of rapidity

variables for standard transverse momentum cuts, dijets resulting from QCD processes will preferentially populate the large rapidity region, while the new processes generate events more uniformly distributed in the entire rapidity region. To analyze the details of the rapidity space the DØ Collaboration [13] introduced a new parameter R, the ratio of the number of events, in a given dijet mass bin, for both rapidities $|y_1|, |y_2| < 0.5$ and both rapidities $0.5 < |y_1|, |y_2| < 1.0$ [14]. In Fig. 2 we compare the results from a full CMS detector simulation of the ratio R [15], with predictions from LO QCD and model-independent contributions to the q^*, g^* and C^* excitations. For an integrated luminosity of 10 fb^{-1} the LO QCD contributions with $\alpha_{\rm QCD} = 0.1$ (corresponding to running scale $\mu \approx M_s$) are within statistical fluctuations of the full CMS detector simulation [16]. Since one of the purposes of utilizing NLO calculations is to fix the choice of the running coupling, we take this agreement as rationale to omit loops in QCD and in string theory. It is clear from Fig. 2 that incorporating NLO calculation of the background and the signal would not significantly change the large deviation of the string contribution from the QCD background. It is noteworthy that although not included in the present analysis, the signal due to $qq \to qq$, with Regge recurrences and Kaluza-Klein excitations exchanged in the t- and u-channels, could yield a small departure from the QCD value of R outside the resonant region. In an optimistic scenario, measurements of this modification could shed light on the D-brane structure of the compact space. It could also serve to differentiate between a stringy origin for the resonance as opposed to an isolated structure such as a Z', which would not modify R outside the resonant region [17].

Before closing, we discuss the impact of Tevatron data on generic D-brane constructions. To do so, we compute the cross section ratio, in a given dijet mass bin, for both rapidities satisfying $|y_1|, |y_2| < 0.5$ and $0.5 < |y_1|, |y_2| < 1.0$, respectively. We use these results to calculate the ratio R, which is shown in Fig. 2. We can essentially read off from the figure that values of $M_s < 700$ GeV are excluded at an extremely high CL. Unfortunately, the dijet mass resolution is not enough to clear up the resonant structure for larger M_s. For example, at first sight the string prediction for $M_s = 1$ TeV seems to depart from the data in the last dijet mass bin. To ascertain any possible deviation, we integrated the cross section over the last inavriant mass bin ($\sigma(0 < |y_1|, |y_2| < 0.5) \simeq 125$ fb, $\sigma(0.5 < |y_1|, |y_2| < 1) \simeq 147$ fb) and estimated an average value of $R = 0.86$ that is in agreement with DØ data [13] at the 1σ level. One should keep in mind that at the Tevatron the valence quark contribution $q\bar{q} \to q\bar{q}$ is presumably an important component of the signal. However, in spite of its importance, we are unable to include this contribution without invoking a specific compactification scenario [18].

Conclusions: In D-brane constructions, the full-fledged string amplitudes supplying the dominant contributions to dijet cross sections are completely independent of the details of compactification. If the string scale is in the TeV range, such extensions of the standard model can be of immediate phenomenological interest. In this Letter we have made use of the amplitudes evaluated near the first resonant pole to determine the discovery potential at LHC for the first Regge excitations of the quark and gluon. We have found that, remarkably, the reach of LHC ($S/N = 210/42$) after a few years of running can be as high as 6.8 TeV [19]. Even after the first 100 pb^{-1} of integrated luminosity, string scales as high as 4.0 TeV can be discovered with $S/N = 55/6$. For string scales as high as 5.0 TeV, observations of resonant structures in $pp \to \gamma +$ jet can provide interesting corroboration for stringy physics at the TeV-scale.

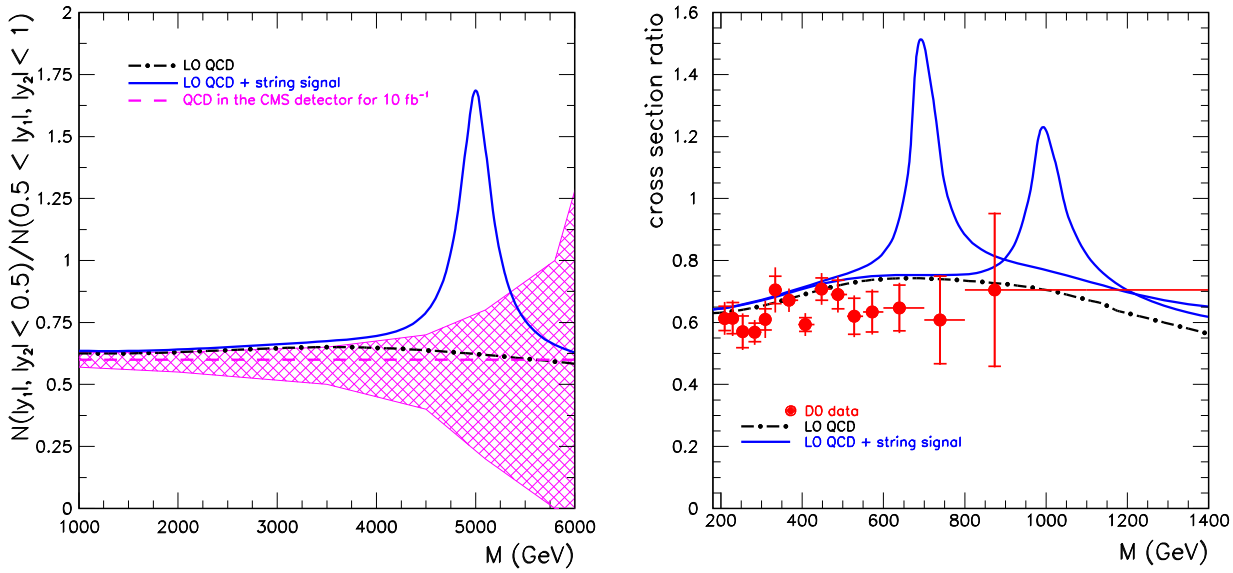

FIG. 2: *Left panel:* For a luminosity of 10 fb^{-1}, the expected value (dashed line) and statistical error (shaded region) of the dijet ratio of QCD in the CMS detector [15] is compared with LO QCD (dot-dashed line) and LO QCD plus lowest massive string excitation at a scale $M_s = 5$ TeV. *Right panel:* Ratio of dijet invariant mass cross sections for rapidities in the interval $0 < |y_1|, |y_2| < 0.5$ and $0.5 < |y_1|, |y_2| < 1$. The experimental points (solid circles) reprtoted by the DØ Collaboration [13] are compared to a LO QCD calculation indicated by a dot-dashed line. The ratio of the string + LO QCD invariant mass cross section, in the same rapidity intervals, is also shown as a solid line for $M_s = 700$ GeV and $M_s = 1$ TeV. The error bars show the statistical and systematic uncertainties added in cuadrature, and the crossbar shows the size of the statistical error.

Acknowledgments

L.A.A. is supported by the U.S. National Science Foundation and the UWM Research Growth Initiative. H.G. is supported by the U.S. National Science Foundation Grants No PHY-0244507 and PHY-0757959. The research of D.L. and St.St. is supported in part by the European Commission under Project MRTN-CT-2004-005104. The research of T.R.T. is supported by the U.S. National Science Foundation Grants PHY-0600304, PHY-0757959 and by the Cluster of Excellence "Origin and Structure of the Universe" in Munich, Germany. He is grateful to Arnold Sommerfeld Center for Theoretical Physics at Ludwig–Maximilians–Universität, and to Max–Planck–Institut für Physik in München, for their kind hospitality. Any opinions, findings, and conclusions or recommendations expressed in this material are those of the authors and do not necessarily reflect the views of the National Science Foundation.

[1] L. A. Anchordoqui, H. Goldberg, S. Nawata and T. R. Taylor, Phys. Rev. Lett. **100**, 171603 (2008) [arXiv:0712.0386 [hep-ph]].

[2] L. A. Anchordoqui, H. Goldberg, S. Nawata and T. R. Taylor, Phys. Rev. D **78**, 016005 (2008)

[arXiv:0804.2013 [hep-ph].]

[3] L. A. Anchordoqui, H. Goldberg and T. R. Taylor, arXiv:0806.3420 [hep-ph]. In that paper, the particles designated as G, G^*, C^{0*} correspond to g, g^*, C^* in the present paper.

[4] D. Lüst, S. Stieberger and T.R. Taylor, arXiv:0807.3333 [hep-th].

[5] N. Arkani-Hamed, S. Dimopoulos and G. R. Dvali, Phys. Lett. B **429**, 263 (1998) [arXiv:hep-ph/9803315].

[6] I. Antoniadis, N. Arkani-Hamed, S. Dimopoulos and G. R. Dvali, Phys. Lett. B **436**, 257 (1998) [arXiv:hep-ph/9804398].

[7] For a review, see: R. Blumenhagen, B. Kors, D. Lüst and S. Stieberger, Phys. Rept. **445**, 1 (2007) [arXiv:hep-th/0610327].

[8] G. Veneziano, Nouvo Cimento A **57**, 190 (1968).

[9] A. Bhatti *et al.*, arXiv:0807.4961 [hep-ex].

[10] J. Pumplin, D. R. Stump, J. Huston, H. L. Lai, P. Nadolsky and W. K. Tung, JHEP **0207**, 012 (2002) [arXiv:hep-ph/0201195].

[11] G. L. Bayatian *et al.* [CMS Collaboration], J. Phys. G **34** 995 (2007); W. W. Armstrong *et al.* [ATLAS Collaboration], CERN/LHCC 94-43.

[12] The approximate equality of the background due to misidentified π^0's and the QCD background, across a range of large p_T^γ as implemented in Ref. [2], is maintained as an approximate equality over a range of invariant γ-jet invariant masses with the rapidity cuts imposed.

[13] B. Abbott *et al.* [D0 Collaboration], Phys. Rev. Lett. **82**, 2457 (1999) [arXiv:hep-ex/9807014].

[14] An illustration of the use of this parameter in a heuristic model where standard model amplitudes are modified by a Veneziano formfactor has been presented by P. Meade and L. Randall, JHEP **0805**, 003 (2008) [arXiv:0708.3017 [hep-ph]].

[15] The synthetic population was generated with Pythia, passed through the full CMS detector simulation and reconstructed with the ORCA reconstruction package; S. Esen and R. Harris, CMS Note 2006/071.

[16] Note that the string scale is an optimal choice of the running scale which should normally minimize the role of higher loop corrections.

[17] Because of the high multiplicity of the angular momenta (up to $J = 2$), the rapidity distribution of the decay products of string excitations would differ significantly from those following decay of a Z' with $J = 1$. With higher statistics, isolation of lowest massive Regge excitations from Kaluza-Klein replicas (with $J = 2$) may also be possible.

[18] Four fermion channels were used previously to obtain model dependent bounds on M_s. See e.g., S. Cullen M. Perelstein and M. E. Peskin, Phys. Rev. D **62**, 055012 (2000) [arXiv:hep-ph/0001166]; P. Burikham, T. Figy and T. Han, Phys. Rev. D **71**, 016005 (2005) [Erratum-ibid. D **71**, 019905 (2005)] [arXiv:hep-ph/0411094]; K. Cheung and Y. F. Liu, Phys. Rev. D **72**, 015010 (2005) [arXiv:hep-ph/0505241].

[19] This intersects with the range of string scales consistent with correct weak mixing angle found in the model of I. Antoniadis, E. Kiritsis and T. N. Tomaras, Phys. Lett. B **486**, 186 (2000) [arXiv:hep-ph/0004214].